Journal of Materials Chemistry B

Accepted Manuscript

ROYAL SOCIETY OF CHEMISTRY

www.rsc.org/materialsB

Table of Content entry

A dual secured nano-melittin system fully retains the wide-spectrum anticancer efficacy of melittin, while quenching its lytic activity for red blood cells.

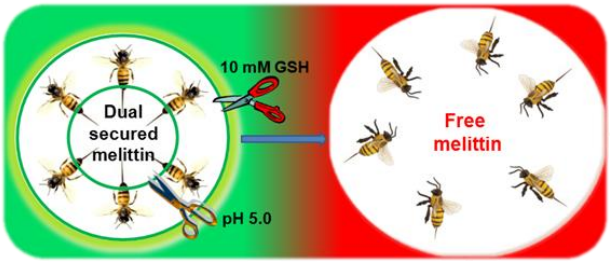

Journal Name

RSCPublishing

ARTICLE

Dual secured nano-melittin for safe and effective eradicating cancer cells†

Cite this: DOI: 10.1039/x0xx00000x

Bei Cheng,‡ Bindu Thapa,‡ Remant K.C. and Peisheng Xu*

Received 00th January 2012,
Accepted 00th January 2012

DOI: 10.1039/x0xx00000x

www.rsc.org/

Clinical application of natural and synthetic amphipathic peptides (e.g., melittin) for cancer therapy is hindered by their notorious side effect, lysing red blood cells. To safely deliver a therapeutic peptide to the tumor tissue and kill cancer cells, we developed an environment-sensitive peptide delivery system, dual secured nano-sting (DSNS), through the combination of a zwitterionic glycol chitosan and disulfide bonds. Melittin loaded DSNS could kill almost 100% of MCF-7, HCT-116, SKOV-3, and NCI/ADR-RES (multidrug resistant) cancer cells at the concentration of 5 μM, while not showing hemolytic effect.

Introduction

The host defense amphipathic peptides found in eukaryotic cells have diverse activities in human and other species originating from their antibiotic, anticancer and anti-inflammatory activities.[1] These peptides oligomerize with phospholipids in cell membrane, result in pore formation, and subsequently cause cell death. In addition, they act in a similar way on the membranes of internal organelles after intracellular transport, and induce cell apoptosis.[2] Amphipathic peptides have been explored for cancer chemotherapy because of their wide-spectrum lytic properties. Melittin is one of the most promising amphipathic water-soluble α-helical cationic polypeptide and is derived from toxin of honey bee *Apis melllifera*.[3] Melittin partitions into and moves laterally in the cell membranes as monomers, followed by oligomerization into toroidal structures, forming pores which results in cell death.[3-4] Furthermore, most recent research showed that melittin can induce cancer cell apoptosis through the inhibition of JAK2/STAT3 pathway.[5] It is worth mentioning that melittin also suppresses the constitutively activated NF-κB, which is partially responsible for the development of drug resistance in cancer cells.[6] It is a very attractive cancer therapeutic agent, because cancer cells are less likely to develop resistance to cytolytic peptides.[1a, 7]

Despite all of these advantages, its non-specific cytolytic activity could lead to off-target effects such as hemolysis (lysis of red blood cells) when administrated intravenously. Besides that, positively charged peptide could be cleared from blood circulation rapidly by the reticuloendothelial system (RES) system.[8] Several groups developed melittin delivery systems either by covalently fusing melittin with receptor-targeted peptide motifs or through physically encapsulating it into liposomes or polymer nanoparticles to attenuate its hemolytic effect while achieving therapeutic efficiency comparable to free melittin.[9] Compared with free melittin, their anticancer efficacies were significantly decreased for the encapsulated form. Until recently, Soman et al. developed a liposome based melittin nanocarrier ("nanobee"), which showed promising results in inhibiting the growth of melanoma tumors.[10] Despite the encouraging outcome of "nanobee", they also found that "nanobee" was about five-fold less effective as that of melittin for the tested cancer cells.

An ideal melittin carrier should be able to completely quench its hemolytic activity while fully retaining its advantages, including wide spectrum and potent anticancer ability. To solve this dilemma, we rationally designed a melittin delivery system by integrating a zwitterionic glycol chitosan and disulfide bonds. Due to its zwitterionic property, succinic anhydride modified glycol chitosan (SA-GCS) shows negative surface charges at physiological pH. Positively charged melittin can form complexes with SA-GCS through the electrostatic effect. The complex will be further stabilized through disulfide crosslinking to yield dual secured nano-sting (DSNS) by aerial oxidation (Scheme 1).

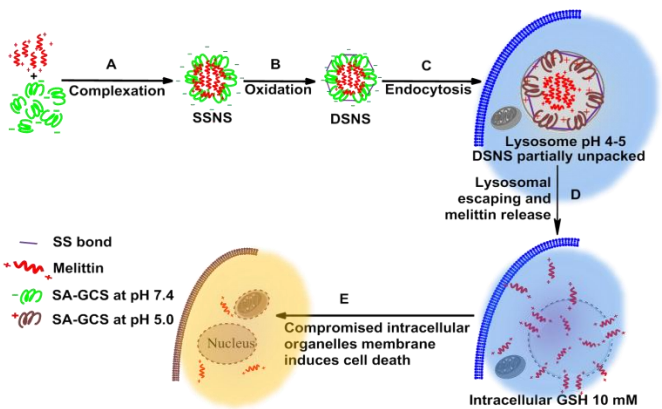

Scheme 1. Schematic illustration of the formation and intracellular pathway of DSNS.

Results and discussion

Synthesis of thiolated zwitterionic glycol chitosan

The zwitterionic glycol chitosan was synthesized from glycol chitosan by amidation with succinic anhydride. First, glycol chitosan was depolymerized by potassium persulfate according to the literature and purified by dialysis against DI water.[11] The resulting polymer has a molecular weight of 28 kDa and PDI of 1.38 (Fig. S1†). After that, glycol chitosan was amidized according to our previously published method with succinic anhydride (Fig. S2†).[8,12] SA-GCS showed negative surface charge at pH 7.4, and positive surface charge at pH below its isoelectric point (IEP) (Fig. 1B). Furthermore, the IEP of the amidized glycol chitosan can be tuned by adjusting the feeding ratio of succinic anhydride and glycol chitosan. To introduce free thiol groups, SA-GCS was reacted with N-succinimidyl 3-[2-pyridyldithio]-propionate (SPDP) and subsequently cleaved with tris(2-carboxyethyl)phosphine (TCEP) to achieve thiolated amidized glycol chitosan (SA-GCS-SH) (Fig. 1A). DTNB assay showed that each polymer chain contains 8.7 free SH groups. The IEP of the SA-GCS slightly decreased after the thiolation (Fig. 1B).

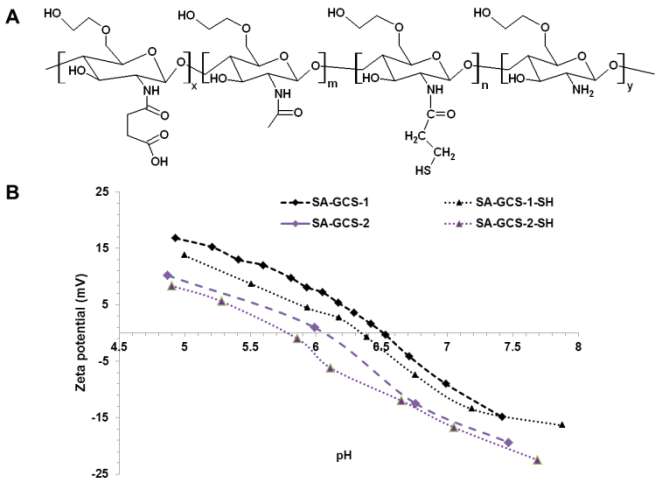

Fig. 1 The structure of SA-GCS-SH (A) and the surface charges of SA-GCS and SA-GCS-SH at different pHs (B).

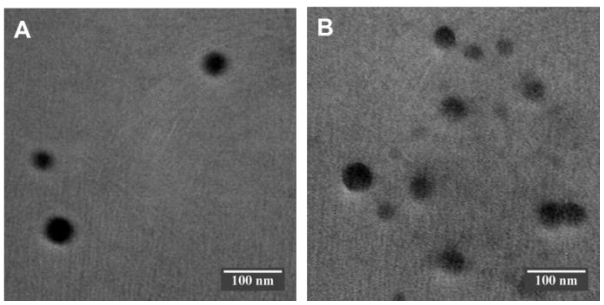

Fig. 2 Transmission electron microscopy images of SSNS (A) and DSNS (B). Scale bars are 100 nm.

Fabrication and characterization of melittin-polymer complexes

To verify that zwitterionic glycol chitosan can form complexes with positively charged melittin, we fabricated the single secure nano-sting (SSNS) by mixing SA-GCS with melittin at pH 7.4 for 2 h at room temperature. The binding efficiency for SA-GCS was determined by measuring the fluorescence intensity of the tryptophan residue of melittin at λ_{EX}: 280nm, λ_{EM}: 350 nm. Fluorescence measurement showed that with the increase of SA-GCS polymer, the detectable free melittin gradually decreases and achieved 100% encapsulation at the polymer to melittin ratio (W/W) of 40 (Fig. S3†).

To further stabilize the complex, inhibit its premature release of melittin, and eliminate its potential side effect, we substituted the SA-GCS with SC-GCS-SH and aerially oxidized the complexe to promote the formation of disulfide bond among the SA-GCS-SH polymers to achieve so called dual secured nano-sting (DSNS). Since safety is an essential requirement for melittin related delivery, polymer to melittin ratio (W/W) of 200 was selected to ensure that no free melittin was remaining after the formation of the complexes. The formation of DSNS was confirmed by dynamic light scattering (DLS) (Fig. S4†) and transmission electron microscopy (TEM) (Fig. 2). The hydrodynamic size of SSNS (220.2 nm, PDI: 0.191) was slightly increased to 223.4 nm after oxidation (PDI: 0.161). The size determined by DLS was larger than that obtained by TEM. This is because TEM measured the size of solid particles while DLS measured the hydrodynamic size of particles which includes the water layer surrounding a particle. This slight size difference between SSNS and DSNS reflected the size decrease and increase due to the formation of intra-particle and inter-particle crosslinking, respectively. Surface charge of the both nano-complexes at pH 7.4 was slightly negative (Fig. S5†), which will help the nano-complexes escape from the detecting of reticuloendothelial system and take advantage of the enhanced permeability and retention effect (EPR) of tumor tissue.[13] HPLC confirmed that no any free melittin existed in the particle suspensions of SSNS and DSNS (Fig. S6†).

Investigate the pH responsiveness of nano-complexes by FRET

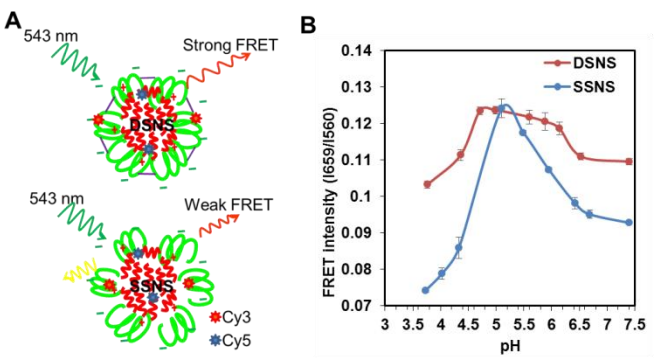

Fig. 3 The Schematic of FRET produced by DSNS and SSNS (A) and the measured FRET intensities of DSNS and SSNS at different pHs (B).

To evaluate the stability of SSNS and DSNS, Förster resonance energy transfer (FRET) technology was employed.[14] Before the fabrication of SSNS and DSNS, melittin and zwitterionic polymer were conjugated with Sulfo-Cy5-NHS and Cy3-NHS, respectively. Cy5-melittin was mixed with Cy3-SA-GCS and Cy3-SA-GCS-SH to achieve SSNS and DSNS, respectively (Fig. 3A). DSNS exhibited a higher FRET signal than SSNS (Fig. 3B) at pH 7.4, indicating that DSNS was tighter than SSNS. To evaluate the nano-sting stability at different pH environments, FRET signal was recorded in the pH range from 7.4 to 3.7. As the pH shifting from 7.4 to the IEPs of the polymers, the FRET intensities of both SSNS and DSNS increased and reached maximum at the pH close to the IEPs of the polymers, indicating the formation of more condensed nanoparticles. Similar to other zwitterionic macromolecules, SA-GCS showed lowest solubility at its IEP. The formation of water insoluble polymer would cause the condensation of SSNS and DSNS, and resulted in

the highest FRET signal. SA-GCS displayed positive surface charge at pH lower than its IEP (Fig. 1B), which would induce the repulsion between SA-GCS and positively charged melittin, similar to the scenario of nano-complex inside lysosome (Scheme 1). As expected, both SSNS and DSNS displayed reduced FRET signal when environment pH was further decreased. At the pH of 3.7, SSNS showed a FRET intensity far less than that at pH 7.4, indicating the dissociation of nanoparticle. By contrast, the lowest FRET intensity DSNS reached at pH 3.7 was still higher than that of SSNS at pH 7.4, suggesting that the formed disulfide bonds did restrict melittin from premature release upon the fluctuation of pH. There was one pH unit left shift of the FRET curve from their corresponding IEPs, which we think was due to the lag response of nano-complexes to the change in environmental pH. The dual secured effect was also evidenced by the slower melittin release from DSNS than SSNS, as well as more melittin released at pH 5.0 than pH 7.4 (Fig.S7†).

Investigate the hemolytic activity of nano-complexes

To validate that the combination of zwitterionic polymer coating and disulfide crosslinking can effectively quench the hemolytic activity of melittin in DSNS, a hemolytic assay was carried out. SSNS and DSNS were incubated with red blood cells (RBCs) in PBS (pH 7.4) first, followed by centrifugation to separate the intact RBCs from the released hemoglobin. As shown in Fig. 4A, melittin lysed almost all RBCs at the concentration of 1 μM. The formation of SSNS partially inhibited the hemolytic activity of melittin. In contrast, there was no detectable red color in the supernatant of RBCs incubated with DSNS at the melittin concentration of 5 μM. The hemolytic activities of SSNS and DSNS were further quantified by UV spectrophotometer. Fig. 4B showed that free melittin was highly lytic to RBCs, lysed almost 100% RBCs at 2 μM, which is the major obstacle for its clinical application. The hemolytic activity of melittin in SSNS was significantly quenched after its complexation with zwitterionic glycol chitosan. The residual hemolytic activity indicated that some melittin was released when incubating with RBCs. Further stabilized through the formation of disulfide bonds, DSNS did not show any hemolytic activity at 2 μM and only caused very few RBCs lyses at the concentration of 5 μM. Therefore, we proved that SSNS was safer than free melittin, while DSNS was almost non-toxic to RBCs up to the melittin concentration of 5 μM in pH 7.4 buffer.

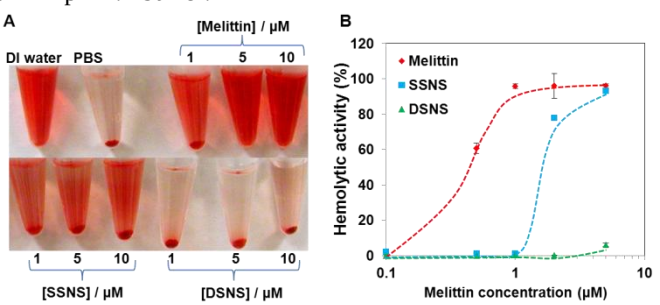

Fig. 4 Images of RBCs after hemolytic assay (A) and the hemolytic activity of melittin, SSNS, and DSNS (B).

To investigate the intracellular membrane lytic activity of SSNS and DSNS, RBCs were co-incubated with melittin, SSNS, and DSNS in PBS (pH 5.0) buffer and PBS (pH 7.4) supplemented with 10 mM glutathione (GSH) to mimic the environments in the acidic lysosome and reducing cytosol, respectively. Acidic pH and reducing environment quenched the hemolytic activity of melittin (Fig. 5), which is consistent with others' observation.[15] SSNS at the concentration of 0.5 and 1.0 μM displayed much higher hemolytic activities in acidic pH than that in pH 7.4, suggesting the release of free melittin at low pH, which was consistent with our FRET observation in Fig. 3B. In contrast, because of the restraint of disulfide bonds, acidic stimulus couldn't trigger the release of melittin from DSNS (Fig. 3B), and induced only slightly more RBCs lysis (Fig. 5). As expected, the addition of 10 mM GSH to pH 7.4 buffer greatly enhanced DSNS's hemolytic activity, reached the similar level as that of SSNS at the concentration of 2 and 5 μM (Fig. 5). Furthermore, the hemolytic activity of DSNS was investigated in 50% serum containing buffer to mimicking blood. Fig. S8† revealed that DSNS was also stable in blood simulating buffer, not causing RBC lysis. Based on these observations, we validated that DSNS should be safe during circulating in the blood stream while effectively lysing intracellular organelles as illustrated in Scheme 1E.

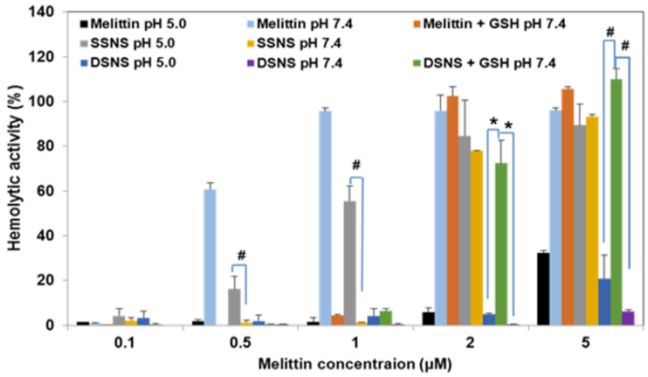

Fig. 5 Hemolytic activity of melittin, SSNS, and DSNS at different pHs and redox potential conditions. * p< 0.05 and # p< 0.01 (unpaired Student's t-test).of RBCs after hemolytic assay (A) and the hemolytic activity of melittin, SSNS, and DSNS (B).

Cellular uptake of nano-complexes

To investigate how the stability of nano-complexes affects their cellular uptake, confocal microscopy was employed. SSNS and DSNS were fabricated as described above except that Cy3-SA-GSC was used instead of SA-GCS. More red spots were detected in cells treated with DSNS than SSNS (Fig. S9†), which suggested that more DSNS nano-complexes entered cancer cells intact than their SSNS counterparts, while some SSNS had dissociated before endocytosis, evidenced by less Cy3 labeled SA-GCS uptake. Since DSNS was more stable than SSNS, as shown in Fig. 3 and further prove by Fig. 4, DSNS won't premature release melittin when contacting with serum protein and red blood cell (Fig. S9†). In contrast, SSNS was only stabilized by the electrostatic effect, which can be dissociated by the competing effect of serum protein. Therefore, more DSNS entered cancer intact than SSNS.

Cell killing effect of nano-complexes

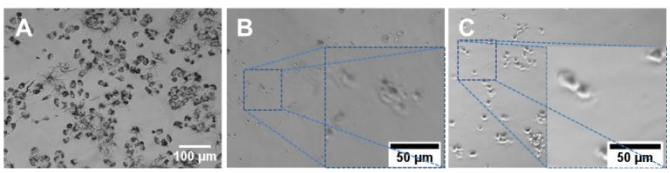

Fig. 6 The morphology of NCI/ADR-RES cells treated with 5 μM melittin. (A) Control, (B) free melittin, (C) DSNS.

Due to the limitation of SSNS associated unwanted hemolytic toxicity, further anticancer efficacy evaluation only included DSNS. NCI/ADR-RES (OVCAR-8 Adriamycin-resistant ovarian) cancer cells were co-cultured with free melittin and

DSNS (melittin concentration of 5 μM) for 24 h.[16] MTT reagent (3-(4,5-Dimethylthiazol-2-yl)-2,5-diphenyltetrazolium bromide) was added after that. Living cells could convert MTT reagent into water insoluble purple crystals (Fig. 6A). The absence of crystals in both melittin and DSNS treated cells indicated that the cells in both treatments were dead. To investigate the possible mechanism of cell death, we examined the cell morphology after treatment. Cells collapsed after co-incubating with free melittin and lost its original shape (Fig. 6B). In contrast to its free melittin treated counterpart, cells in Fig. 6C kept their intact shape after DSNS treatment. Since melittin can attack cancer cells by forming pore structures on cell membrane,[17] we postulate the cell death in melittin treatment group was mainly due to the loss of cell membrane integrity. DSNS, due to the dual-secured mechanism, could effectively enter cancer cells (Fig. S9†) and release melittin intracellularlly (Scheme 1 and Fig. 5). Therefore, we postulate that DSNS treated cells were killed mainly due to the compromised membranes of internal organelles (e.g., mitochondria). After co-incubating with DSNS and followed by JC-1 staining, the emerging green fluorescence signals in DSNS treated cell (Fig. S10†) confirmed that cancer cells were killed due to mitochondria damage.

The anticancer efficacy of DSNS was further quantitatively evaluated in four types of cancer cells, HCT-116 colon cancer cells, MCF-7 breast cancer cells, SKOV-3 ovarian cancer cells, and NCI/ADR-RES/OVCAR-8 ovarian (Adriamycin-resistant) cancer cells by MTT assay. As expected, both free melittin and DSNS showed dose-dependent cytotoxicity and could kill 100% of the cancer cells at a high dose (Fig. 7). It is worthwhile to note that DSNS was more effective in killing HCT-116 cells. DSNS killed 100% of HCT-116 cells at the melittin concentration of 5 μM, at which free melittin could only kill 76% cancer cells (Fig. 7A). Most importantly, DSNS only showed negligible hemolytic activity at the same concentration (Fig. 4B). A similar anticancer effect was observed for MCF-7 breast cancer cells and SKOV-3 ovarian cancer cells (Fig. 7B and 7C). Furthermore, we also found that DSNS killed 100% of Adriamycin-resistant ovarian cancer cells at the melittin concentration of 5 μM (Fig. 7D), which have developed multidrug resistance. Altogether, we proved that anticancer capacity of melittin of DSNS, in contrast to other melittin carrier systems,[7, 9a] was fully retained. In addition, the polymer carrier itself was not toxic for all four tested cell lines (Fig. S11†).

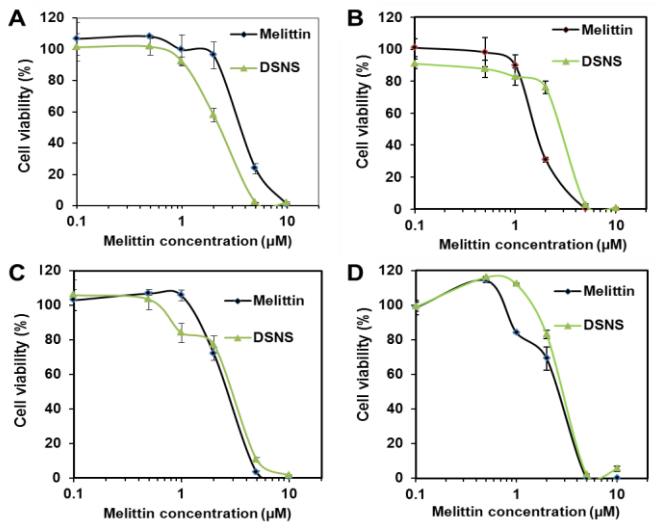

Fig. 7 Cytotoxicity of melittin and DSNS for (A) HCT-116 colon cancer cell, (B) MCF-7 breast cancer cell, (C) SKOV-3 ovarian cancer cell, and (D) NCI/ADR-RES (OVCAR-8 ovarian Adriamycin-resistant) cancer cell. Cells were incubated with melittin and DSNS at the melittin concentration from 0.1 to 10 μM for 24 h. Data represent mean ± SD, n=3.

Conclusions

In summary, we have fabricated DSNS nano-complexes through the electrostatic absorption of zwitterionic glycol chitosan and disulfide crosslinking to deliver melittin for cancer therapy. The hemolytic activity of melittin in DSNS could be completely quenched by our unique dual secured design. Due to the pH and redox potential dual responsiveness of DSNS, the wide-spectrum anticancer activity of melittin was fully retained, eradicating 100% of four types of tested cancer cell lines, including a drug resistant cell line. These studies demonstrated that the combination of zwitterionic polymer and redox sensitive bonds offers a new strategy for safe and effective therapeutic peptide delivery. The next step of research would be adding cancer cell targeting ligands, such as folic acid, anisamide, and disaccharide moiety of bleomycin,[18] to the DSNS to further enhance its tumor specificity.

Acknowledgements

The authors want to thank the American Cancer Society Institutional Research Grant (ACS-IRG), the ASPIRE award from the Office of the Vice President for Research of The University of South Carolina, the Center for Targeted Therapeutics (1P20 GM109091), and the Center for Colon Cancer Research (5P30 GM103336-02) for financial support.

Notes and references

Department of Drug Discovery and Biomedical Sciences, South Carolina College of Pharmacy, University of South Carolina, 715 Sumter St., Columbia, SC 29208, USA. E-mail: xup@sccp.sc.edu; Fax: +1-803-777-8356; Tel: 1-803-777-0075

‡ B.C. and B.T. contributed equally.

† Electronic Supplementary Information (ESI) available: [Experimental procedures for the synthesis of thiolated amidized glycol chitosan, nano-complexes preparation and characterization, FRET measurement, release kinetics, hemolytic assay, confocal microscopy, and cytotoxicity assay]. See DOI: 10.1039/b000000x/

1 (*a*) D. W. Hoskin, A. Ramamoorthy, *Biochim. Biophys. Acta*, 2008, **1778**, 357-375; (*b*) N. Papo, Y. Shai, *Cell Mol. Life Sci.*, 2005, **62**, 784-790.

2 (*a*) L. Yang, T. A. Harroun, T. M. Weiss, L. Ding, H. W. Huang, *Biophys. J.*, 2001, **81**, 1475-1485; (*b*) M. T. Lee, W. C. Hung, F. Y. Chen, H. W. Huang, *Proc. Natl. Acad. Sci. U. S. A.*, 2008, **105**, 5087-5092.

3 M. T. Tosteson, D. C. Tosteson, *Biophys. J.*, 1981, **36**, 109-116.

4 (*a*) W. F. DeGrado, G. F. Musso, M. Lieber, E. T. Kaiser, F. J. Kezdy, *Biophys. J.*, 1982, **37**, 329-338; (*b*) K. A. Brogden, *Nature Rev. Microbiol.*, 2005, **3**, 238-250; (*c*) J. F. Popplewell, M. J. Swann, N. J. Freeman, C. McDonnell, R. C. Ford, *Biochim. Biophys. Acta*, 2007,**1768**, 13–20.

5 M. Jo, M. H. Park, P. S. Kollipara, B. J. An, H. S. Song, S. B. Han, J. H. Kim, M. J. Song, J. T. Hong, *Toxicol. Appl. Pharm.*, 2012, **258**, 72-81.

6 M. H. Park, M. S. Choi, D. H. Kwak, K.-W. Oh, D. Y. Yoon, S. B. Han, H. S. Song, M. J. Song, J. T. Hong, *Prostate*, 2011, **71**, 801-812.

7 H. Pan, N. R. Soman, P. H. Schlesinger, G. M. Lanza, S. A. Wickline, *WIREs Nanomed. Nanobiotechnol.*, 2011, **3**, 318-327.

8 P. Xu, E. A. Van Kirk, Y. Zhan, W. J. Murdoch, M. Radosz, Y. Shen, *Angew. Chem. Int. Ed .Engl.*, 2007, **46**, 4999-5002.

9 (*a*) C. Huang, H. Jin, Y. Qian, S. Qi, H. Luo, Q. Luo, Z. Zhang, *ACS Nano*, 2013, **7**, 5791-5800; (b) C. Leuschner, W. Hansel, *Curr. Pharm. Des.*, 2004, **10**, 2299-2310; (c) W. Hansel, C. Leuschner, F. Enright, *Mol. Cell Endocrinol.*, 2007, **269**, 26-33; (d) C. S. Kumar, C. Leuschner, E. E. Doomes, L. Henry, M. Juban, J. Hormes, *J. Nanosci. Nanotechnol.*, 2004, **4**, 245-249.

10 N. R. Soman, S. L. Baldwin, G. Hu, J. N. Marsh, G. M. Lanza, J. E. Heuser, J. M. Arbeit, S. A. Wickline, P. H. Schlesinger, *J. Clin. Invest.*, 2009, **119**, 2830-2842.

11 D. K. Knight, S. N. Shapka, B. G. Amsden, *J. Biomed. Mater. Res. A*, 2007, **83A**, 787-798.

12 P. Xu, G. Bajaj, T. Shugg, W. G. Van Alstine, Y. Yeo, *Biomacromolecules*, 2010, **11**, 2352-2358.

13 (*a*) K. Xiao, Y. Li, J. Luo, J. S. Lee, W. Xiao, A. M. Gonik, R. G. Agarwal, K. S. Lam, *Biomaterials*, 2011, **32**, 3435-3446; (*b*) K. C. R. Bahadur, B. Thapa, P. Xu, *Macromol. Biosci.*, 2012, **12**, 637-646.

14 (*a*) Y. P. Ho, H. H. Chen, K. W. Leong, T. H. Wang, *J. Control. Release*, 2006, **116**, 83-89; (*b*) C. A. Alabi, K. T. Love, G. Sahay, T. Stutzman, W. T. Young, R. Langer, D. G. Anderson, *ACS Nano*, 2012, **6**, 6133-6141.

15 (*a*)Y.-X. Tan, C. Chen, Y.-L. Wang, S. Lin, Y. Wang, S.-B. Li, X.-P. Jin, H.-W. Gao, F.-S. Du, F. Gong, S.-P. Ji, *J. Gene Med.*, 2012, **14**, 241-250; (*b*) N. J. Baumhover, K. Anderson, C. A. Fernandez, K. G. Rice, *Bioconjugate Chem*., 2010, **21**, 74–83.

16 (*a*) D. A. Scudiero, A. Monks, E. A. Sausville, *J. Natl. Cancer Inst.*, 1998, **90**, 862-862; (*b*) L. A. Garraway, H. R. Widlund, M. A. Rubin, G. Getz, A. J. Berger, S. Ramaswamy, R. Beroukhim, D. A. Milner, S. R. Granter, J. Y. Du, C. Lee, S. N. Wagner, C. Li, T. R. Golub, D. L. Rimm, M. L. Meyerson, D. E. Fisher, W. R. Sellers, *Nature*, 2005, **436**, 117-122.

17. M. Lee, T. Sun, W. Hung, H. Huang, *Proc Natl Acad Sci U S A.* 2013,**110**,14243-8.

18. (*a*) H. S. Yoo, T. G. Park, *J. Control. Release*, 2004, **100**, 247–256; (*b*) H. He, A. Cattran, T. Nguyen, A. Nieminen, and P. Xu, *Biomaterials*, 2014, **35**, 9546–9553; (*c*) Z. Yu, R. M. Schmaltz, T. C. Bozeman, R. Paul, M. J. Rishel, K. S. Tsosie, S. M. Hecht, *J. Am. Chem. Soc.*, 2013, **135**, 2883−2886; (*d*) C. Bhattacharya, Z. Yu, M. J. Rishel, S. M. Hecht, *Biochemistry*, 2014, **53**, 3264–3266.